RESPONSE OF A TUNGSTEN CALORIMETER TO FNAL PROTON BEAMS*

D. L. Cheshire, R. W. Huggett, and W. V. Jones
Louisiana State University, Baton Rouge, Louisiana 70803

and

W. K. H. Schmidt and M. Simon
Max Planck Institut fuer Extraterrestrische Physik
D-8046 Garching bei Muenchen, W. Germany

ABSTRACT

A tungsten-scintillator ionization calorimeter of $\sim$ 1000 g/cm^2 total depth has been exposed to 100, 200, and 300 GeV/c proton beams at FNAL. The apparatus included a five layer CsI target upstream from the calorimeter. Preliminary data are described. Results are presented in terms of the cascade development curves and the fraction of the incident energy measured by the apparatus. The resolutions are given as a function of calorimeter depth and as a function of primary energy.

1. INTRODUCTION

A tungsten-scintillator ionization calorimeter which was built as a prototype for a satellite experiment[1] to measure the energy spectra and charge composition of high energy cosmic rays has been exposed to 100, 200, and 300 GeV/c protons at the Fermi National Accelerator Laboratory (FNAL). The same apparatus was exposed to 5, 10, and 15 GeV/c electrons as well as 5, 10, and 15 GeV/c pions at the Stanford Linear Accelerator Center (SLAC)[2] and also to 2.1 GeV/nucleon ^{12}C and ^{16}O beams at the Lawrence Berkeley Laboratory Bevatron.[3] To be reported here are the first results from the FNAL exposure.

Since the data analysis is not yet complete we would like to caution the reader that these are preliminary results. Our primary concern is with the normalization of the experimental data.

Therefore caution is warranted only for normalization of the cascade development curves to be presented as well as for the absolute energies measured by the calorimeter.

2. APPARATUS

The arrangement of the apparatus in the FNAL experiment is shown schematically in Fig. 1. Wire spark chambers SC_1 and SC_2 provided trajectory information which was used for event selection in the data analysis. An event trigger was defined by plastic scintillators S_2 and S_3. The 5 cm diameter plastic scintillators B_1 and B_2 were used to tag beam particles passing through the center of the calorimeter. In some of the data runs a $B_1 \cdot S_2 \cdot S_3 \cdot B_2$ event trigger was used, in which case, signals from B_1 and B_2 were required.

The target consisted of a stack of five CsI (Tℓ) crystal detectors (CsI_1- CsI_5) viewed by separate photomultipliers. Each crystal was 2 cm (9 g/cm^2) thick and was immersed in oil in a plexiglass casing with walls 1 mm thick.

Modules T_1- T_5, which are called high resolution modules (HRM), each consisted of a 13 g/cm^2 thick tungsten layer (95% W, 5% Ni) followed by a 0.65 cm thick sheet of plastic scintillator. Each module was viewed by a separate photomultiplier. Each of the eleven thick modules T_6- T_{16} consisted of four layers of tungsten (total thickness 79 g/cm^2) and three sheets of 0.65 cm thick plastic scintillator arranged in alternating layers, with 26.3 g/cm^2 or 3.7 radiation lengths (r.l.) of tungsten between each pair of scintillators. A photomultiplier on each of the two opposite sides of the module viewed all three scintillators. The signals from the two photomultipliers were added electronically, and the resulting signal was used to determine the response of the module. Thus, although the ionization was sampled every 3.7 r.l., the signal from a module was a measure of the average ionization over the entire module (11.1 r.l.).

3. RESULTS

Cascade Curves. Figure 2 shows for the 300 GeV data, the average number of "equivalent particles" in the cascade as a function of depth in the calorimeter. Separate curves are shown for all incident events and for the subset of events in which the proton had its first interaction near the top (HRM) of the calorimeter.

Localizing the first interactions results in two rather striking features: (1) the cascade maximum contains about twice the number of particles in the maximum of the cascade for all events and (2) the cascade exhibits a pronounced non-smooth behavior just beyond the maximum. The greater average number of particles at the maximum results, of course, from the fact that the curve for all events includes many single particles which have not yet interacted. The explanation for the pronounced peaking in the curve for the localized interactions lies in the high inelasticity as well as in the large ratio of the interaction length to the radiation length for tungsten. Cascades in lighter materials, such as iron, do not show such pronounced non-smooth behavior.

Energy Measurements. Figure 3 shows the distribution of energy measured by the total depth of the calorimeter. The measured energy (E_m) was determined from the number of equivalent particles comprising the cascade in each module of the calorimeter. The energy deposited in each (i^{th}) module was estimated using the relation

$$E_i = \{[(\frac{dE}{dx})_W \cdot t_W] + [(\frac{dE}{dx})_{Sc} \cdot t_{Sc}] + [(\frac{dE}{dx})_{CsI} \cdot t_{CsI}]\} \times N_i, \qquad (1)$$

where N_i is the number of equivalent particles observed in the scintillator layer(s) of the i^{th} module, and t_W, t_{Sc} and t_{CsI} are the respective thicknesses of tungsten, plastic scintillator and CsI in the module. The following average values for the energy loss rate dE/dx of vertically incident sea-level muons were used: 1.64 MeV/(g cm^{-2}) in CsI, 1.55 MeV/(g cm^{-2}) in W, and 2.27 MeV/(g cm^{-2}) in plastic scintillator. These values were calculated

from information presented by Barkas and Berger.[4] For our module configurations, Eq. (1) reduces to $E_i = 15.4\ N_i$, $21.8\ N_i$, and $126.4\ N_i$, respectively, for the CsI, the HRM, and the thick tungsten modules. A sum over all modules gives E_m for an individual event.

In Figs. 4 and 5 are shown the distributions of energy measured by the top half of the calorimeter for the same data used to obtain Fig. 3. The distribution in Fig. 4 is for all 300 GeV protons incident upon the calorimeter, while Fig. 5 represents only those particles which interacted in the HRM. The left peak (one channel wide) in the distribution of Fig. 4 represents particles which penetrated the top half of the calorimeter without interacting. This peak does not appear if the incident protons are required to interact near the top. The width of the distribution in Fig. 4 is somewhat wider than the distribution in Fig. 5.

Energy Resolutions. The dependence of the energy resolution on the calorimeter depth is illustrated in Fig. 6. The two curves represent the normal standard deviations of the measured energy loss distributions for all incident particles (top curve) and for those particles which interacted in the HRM (bottom curve). It is seen that for both cases the resolution improves with depth of the calorimeter, but this improvement is less for particles which interacted near the top. If the depth is sufficiently large, there is not much difference in the energy resolution for the two cases, so that with a deep calorimeter it matters very little where the first interaction of the particle occurs. However, if the calorimeter is shallow, reasonable energy resolution can be obtained only if the particles have interacted and the subsequent electromagnetic cascades have developed.

The data presented in Fig. 7 show the dependence of the energy resolution on primary energy. Results are given for two fixed depths. Both curves are for particles interacting in the HRM of the calorimeter. The lower curve is for the maximum depth, while the upper curve was obtained from the energy deposited in the upper half of the calorimeter. The data points at 5, 10, and 15 GeV are from earlier measurements (using the same apparatus)

made on negatively charged pions at the Stanford Linear Accelerator Center (SLAC). The 300 GeV data are essentially 100% protons, while the 100 and 200 GeV data are for protons contaminated with pions. The pion contaminations are estimated to be 5% and 50%, respectively, at 200 GeV and 100 GeV. Since high energy pions and protons produce very similar cascades, the curves can be taken as representative of protons. Some small differences may exist for the lowest energy of 5 GeV.

REFERENCES

* Research supported by NASA Contract No NAS5-11426, NASA Grant No. NGR 19-001-012, by the U.S. National Science Foundation, and by the German Science Ministry Grant No. WRK-244.

1. J. F. Ormes, V. K. Balasubrahmanyan, T. Bowen, R. W. Huggett, T.A. Parnell, and K. Pinkau, "Composition and Spectra of High Energy Cosmic Rays"- A proposal for an Orbiting Laboratory for the HEAO, GSFC Report No. X-661-71-1 (unpublished).
2. D. L. Cheshire, R. W. Huggett, D. P. Johnson, W. V. Jones, S. P. Rountree, W.K.H. Schmidt, R. J. Kurz, T. Bowen, D. A. DeLise, E. P. Krider, and C. D. Orth, Nucl. Instrum. Methods (in press).
3. D. L. Cheshire, R. W. Huggett, D. P. Johnson, W. V. Jones, S. P. Rountree, S. D. Verma, W.K.H. Schmidt, R. J. Kurz, T. Bowen, and E. P. Krider, Phys. Rev. D 10 (1974) 25.
4. W. H. Barkas and M. J. Berger, "Tables of Energy Losses and Ranges of Heavy Charged Particles", Report 7 of NAS-NRC Publication 1133.

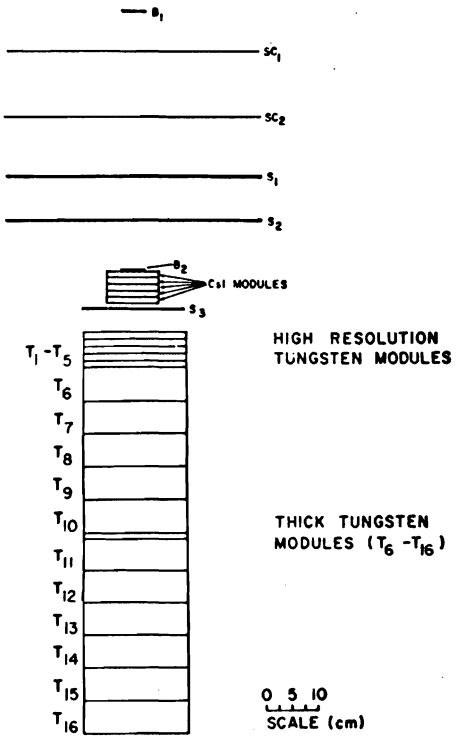

Fig. 1

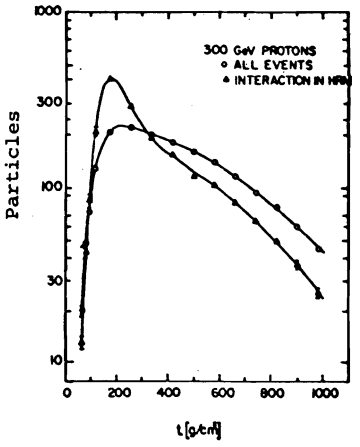

Fig. 2

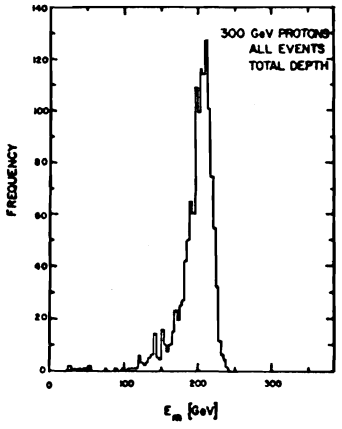

Fig. 3

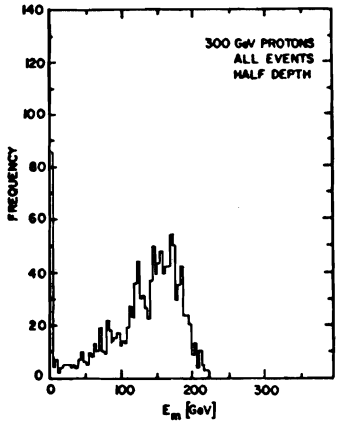

Fig. 4

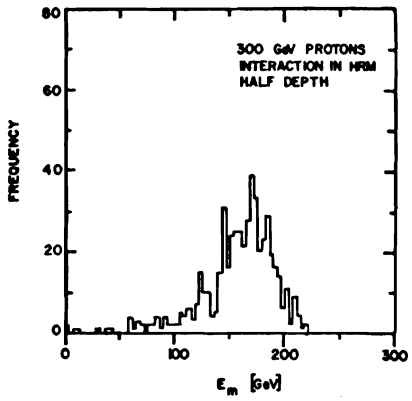

Fig. 5

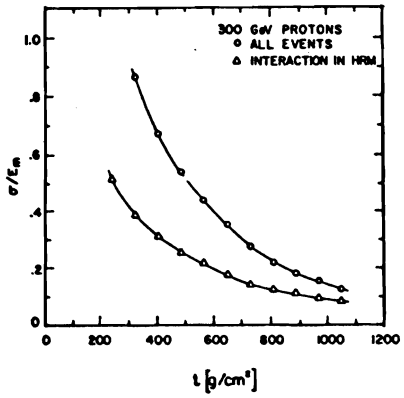

Fig. 6

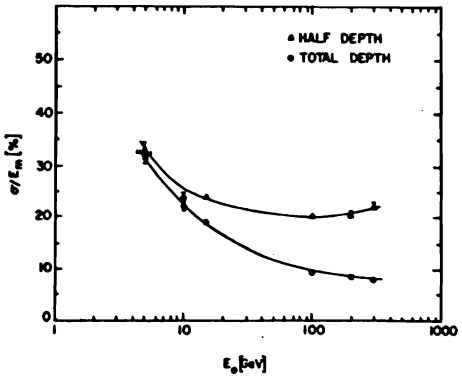

Fig. 7